



HAL
open science

Nonlinear soft-sensors design for unsteady-state VOC afterburners

D. Fissore, David Edouard, Hassan Hammouri, A. Barresi

► **To cite this version:**

D. Fissore, David Edouard, Hassan Hammouri, A. Barresi. Nonlinear soft-sensors design for unsteady-state VOC afterburners. *AIChE Journal*, 2006, 52 (1), pp.282-291. 10.1002/aic.10602 . hal-00091558

HAL Id: hal-00091558

<https://hal.science/hal-00091558>

Submitted on 18 Oct 2010

HAL is a multi-disciplinary open access archive for the deposit and dissemination of scientific research documents, whether they are published or not. The documents may come from teaching and research institutions in France or abroad, or from public or private research centers.

L'archive ouverte pluridisciplinaire **HAL**, est destinée au dépôt et à la diffusion de documents scientifiques de niveau recherche, publiés ou non, émanant des établissements d'enseignement et de recherche français ou étrangers, des laboratoires publics ou privés.

**This document must be cited according to its final version
which is published in a journal as:**

**D. Fissore¹, D. Edouard², H. Hammouri³, A. Barresi¹
"Nonlinear soft-sensors design for unsteady-state VOC afterburners",
American Institute of Chemical Engineers (AIChE) Journal
52, 1 (2006) 282-291**

This final version may be found:

<http://dx.doi.org/10.1002/aic.10602>

All open archive documents of H. Hammouri are available at:

<http://hal.archives-ouvertes.fr/HAMMOURI-HASSAN>

**All open archive documents of H. Hammouri research group (SNLEP)
are available at:**

<http://hal.archives-ouvertes.fr/SNELP>

<http://www.tinyurl.com/SNELP>

The professional web page (Fr/En) of H. Hammouri is:

<http://www.lagep.univ-lyon1.fr/signatures/hammouri.hassan>

1

POLITO Torino Italy

Dip. di Scienza dei Materiali ed Ingegneria Chimica, Politecnico di Torino, 10129 Torino, Italy

<http://www.dismic.polito.it>

2

LGPC-CNRS, CPE-Lyon, 69616 Villeurbanne Cedex, France

<http://www.lgpc.fr>

3

Université de Lyon, Lyon, F-69003, France; Université Lyon 1;

CNRS UMR 5007 LAGEP (Laboratoire d'Automatique et de GENie des Procédés),

43 bd du 11 novembre, 69100 Villeurbanne, France

Tel +33 (0) 4 72 43 18 45 - Fax +33 (0) 4 72 43 16 99

<http://www.lagep.univ-lyon1.fr/> <http://www.univ-lyon1.fr> <http://www.cnrs.fr>

Non-linear soft-sensors design for unsteady-state VOC afterburners

Davide Fissore^{1}, David Edouard², Hassan Hammouri³, Antonello A. Barresi¹*

1. Dipartimento di Scienza dei Materiali ed Ingegneria Chimica, Politecnico di Torino, corso Duca degli Abruzzi 24, 10129 Torino (Italy)

2. LGPC-CNRS, CPE-Lyon, Bat. 308 F, 43 Bd du 11 Novembre 1918, 69616 Villeurbanne Cedex, France

3. LAGEP, UMR 5007, UCBL I, CPE-Lyon, Bat. 308 G, 43 Bd du 11 Novembre 1918, 69616 Villeurbanne Cedex, France

* corresponding author: Davide Fissore, Dipartimento di Scienza dei Materiali ed Ingegneria Chimica, Politecnico di Torino, corso Duca degli Abruzzi 24, 10129 Torino (Italy), phone: +39-011-5644695, fax: +39-011-5644699, e-mail: davide.fissore@polito.it

Abstract

An observer for a reverse-flow reactor, where the combustion of lean VOC mixtures takes place, is designed in this work and it is demonstrated to allow for a quick and reliable estimation of the inlet pollutant concentration and of the outlet reactant conversion from some temperature measurements in the reactor, even when the pollutant concentration in the feed or the pollutant itself change and when the reaction is moving towards the extinction. The results may be used for control purposes, thus avoiding expensive hardware sensors and time consuming on-line measurements.

Keywords: observer; reverse-flow reactor; countercurrent reactor; pseudo-homogeneous model; VOC combustion, state estimation.

Introduction

Forced unsteady-state catalytic reactors were investigated in the past as it was demonstrated that temperature and composition distributions, which cannot be obtained in any steady-state regime, can be achieved by means of forced variations of some operation parameters, thus improving both conversion and selectivity in a wide range of chemical processes (see, for example, Matros and Bunimovich, 1996).

A simple technical solution to get forced unsteady-state operation is the periodic reversal of the feed flowing direction. For an exothermic reaction, the reverse flow reactor (RFR) exhibits a heat trap effect which can be used to achieve and maintain an enhanced reactor temperature compared to a constant flow direction mode of operation. Under periodic flow reversal both ends of the fixed bed are used as regenerative heat exchangers. Since regenerative heat exchange is generally considered simpler and more efficient than recuperative heat exchange, the RFR has found considerable industrial application primarily for the catalytic combustion of organic pollutants in exhaust air, strongly reducing the need of auxiliary fuel to sustain the combustion, except during the start-up (Matros and Bunimovich, 1996; Eigenberger, 1992).

In addition to the intrinsically dynamic behaviour of the RFR, one must deal with external perturbations (in the feed concentration, composition, temperature and flow rate) which may lead either to reactor extinction (and thus to emission of unconverted pollutants) or to catalyst overheating (and thus deactivation). In order to avoid these problems it is necessary to implement some closed-loop control strategy based on the measurement of the inlet concentration (and composition) and the outlet conversion. Dufour et al. (2003) and Dufour and Touré (2004), for example, applied a Model Predictive Control algorithm for the control of a RFR in which the inlet pollutant concentration is known, without discussing how this value is obtained: on-line measurements may be in fact expensive and time consuming, thus introducing a delay in the control loop.

A model-based soft-sensor (observer) can be used to estimate quickly and reliably the feed composition from some temperature measurements in the reactor: the observer combines the knowledge of the physical system (model) with experimental data (some on-line measures) to provide on-line estimates of the sought states and/or parameters. The level of detail of the model is of straightforward importance in characterising the performance of the observer: if a detailed model taking into account finite reversal frequency and reaction kinetics is used, the resulting observer may be useless for the on line application, being too time consuming for a computer. Edouard et al. (2004) designed an observer for a medium scale RFR, using a simplified model which is the extended version of the countercurrent reactor model of Ramdani et al. (2001). The main assumption of their model is that the reaction is instantaneous and under mass-transfer control: this implies that it will be impossible to predict the extinction phenomenon; conversely, the model is independent of any chemical kinetic data. Moreover, this observer was demonstrated to give correct predictions only when the reactor is fully ignited, so that, if we want to use it for control purposes, we may face against catalyst overheating, but not against reactor extinction and pollutant emission. This observer was used by Edouard et al. (2005) in a state-space based control system, proving the efficiency of this approach, even if the application is limited to the case of fully ignited reactor, due to the hypothesis of the model.

The aim of this paper is thus to develop further the approach of Edouard et al. (2004), removing the assumption of instantaneous, mass-transfer controlled reaction: the resulting observer will be able to estimate the inlet concentration and the outlet conversion also when the reactor is moving toward extinction. When the assumption of instantaneous and mass-transfer controlled reaction is removed, the model becomes dependent of the kinetic parameters. Thus the observer can also be used to estimate the kinetic parameters of the reacting mixtures: this may be useful when these parameters change because of catalyst deactivation or changes in the feed composition.

The same system of Edouard et al. (2004) will be considered, being it quite representative of industrial apparatus. The packing is made of two sets of monoliths: a long inert monolith and a short catalytic one. The wide square cross section of the monoliths prevents heat losses over their whole length (Ramdani et al, 2001); conversely, heat loss through the reactor wall takes place between the monoliths in the central chamber where the electrical heater is located and where fresh air can be injected. Figure 1 sketches the main geometrical characteristics of the RFR.

The paper is structured as follows: Section 2 describes the simplified model which was used in the observer design; in Section 3 the fundamentals of the observer design are given, while the validation is given in Section 4.

Modelling of the RFR

The analogy between the countercurrent reactor and the RFR was used in this work to build up a simple model. This analogy was firstly stated by Nieken et al. (1995) and was demonstrated to occur when the switching frequency is infinite. Figure 2 shows a sketch of the countercurrent reactor under study. The basic balance equations are:

$$\lambda_{ax}^S \frac{\partial^2 T_S}{\partial z^2} + \frac{ha_v}{2} (T_{G,1} + T_{G,2} - 2T_S) + a_v (-\Delta H) \frac{r_{S,1} + r_{S,2}}{2} = (1 - \varepsilon) \rho_S c_{p,S} \frac{\partial T_S}{\partial t} \quad (1)$$

$$\alpha \rho_{G,0} v_0 c_{p,G} \frac{\partial T_{G,1}}{\partial z} + ha_v (T_{G,1} - T_S) = 0 \quad (2)$$

$$-\rho_{G,0} v_0 c_{p,G} \frac{\partial T_{G,2}}{\partial z} + ha_v (T_{G,2} - T_S) = 0 \quad (3)$$

$$\alpha \rho_{G,0} v_0 c_{p,G} \frac{\partial \omega_{G,1}}{\partial z} + k_D a_v \rho_G (\omega_{G,1} - \omega_{S,1}) = 0 \quad (4)$$

$$-\rho_{G,0} v_0 \frac{\partial \omega_{G,2}}{\partial z} + k_D a_v \rho_G (\omega_{G,2} - \omega_{S,2}) = 0 \quad (5)$$

$$k_D (\omega_{G,1} - \omega_{S,1}) = M \frac{r_{S,1}}{\rho_G} \quad (6)$$

$$k_D (\omega_{G,2} - \omega_{S,2}) = M \frac{r_{S,2}}{\rho_G} \quad (7)$$

Normalising some variables and assuming that the Nusselt and Sherwood numbers on one hand, and the Schmidt and Prandtl numbers on the other hand, are equal, gives $h = k_D \rho_G c_{p,G}$ and:

$$\frac{1}{P_{ax}} \frac{\partial^2 T_S}{\partial x^2} + P \left(\frac{T_{G,1} + T_{G,2}}{2} - T_S \right) + \frac{a_v (-\Delta H) (H/2) r_{S,1} + r_{S,2}}{\rho_{G,0} v_0 c_{p,G}} \varphi(x) = \tau \frac{\partial T_S}{\partial t} \quad (8)$$

$$\alpha \frac{\partial T_{G,1}}{\partial x} + P (T_{G,1} - T_S) = 0 \quad (9)$$

$$-\frac{\partial T_{G,2}}{\partial x} + P (T_{G,2} - T_S) = 0 \quad (10)$$

$$\alpha \frac{\partial \omega_{G,1}}{\partial x} + P (\omega_{G,1} - \omega_{S,1}) = 0 \quad (11)$$

$$-\frac{\partial \omega_{G,2}}{\partial x} + P (\omega_{G,2} - \omega_{S,2}) = 0 \quad (12)$$

$$P (\omega_{G,1} - \omega_{S,1}) = \frac{Ma_v (H/2)}{\rho_{G,0} v_0} r_{S,1} \quad (13)$$

$$P (\omega_{G,2} - \omega_{S,2}) = \frac{Ma_v (H/2)}{\rho_{G,0} v_0} r_{S,2} \quad (14)$$

where:

$$x = \frac{z}{H/2}, \quad \frac{1}{P_{ax}} = \frac{\lambda_{ax}^s}{\rho_{G,0} v_0 c_{p,G} H/2}, \quad \tau = \frac{(1-\varepsilon) \rho_S c_{p,S} H/2}{\rho_{G,0} v_0 c_{p,G}}, \quad P = \frac{ha_v H/2}{\rho_{G,0} v_0 c_{p,G}} \quad (15)$$

and $\varphi(x)$ accounts for the type of monoliths: $\varphi(x) = 0$ in the inert monoliths ($x < \xi$) and $\varphi(x) = 1$ in the catalytic monoliths ($x \geq \xi$). The boundary conditions for the mass balances are:

$$\begin{cases} x = 0, \omega_{G,1} = \omega_{G,0} \\ x = 1, \alpha \omega_{G,1} = \omega_{G,2} \end{cases} \quad (16)$$

while the boundary conditions for the thermal balances are:

$$\begin{cases} x = 0, T_{G,1} = T_{G,0}, \frac{\partial T_s}{\partial x} = 0 \\ x = 1, (1 + N')(T_{G,2} - T_{G,0}) = \alpha(T_{G,1} - T_{G,0}) + \frac{\dot{Q}_{ext}}{\rho_{G,0} v_0 c_{p,G} S}, \frac{\partial T_s}{\partial x} = 0 \end{cases} \quad (17)$$

where N' is the number of transfer units that accounts for heat loss in the central chamber.

The model given by eq. (8) - (17) is further simplified using the approach of Balakotaiah and Dommeti (1999), thus expressing the gas temperature as a function of the solid temperature: Eq. (9) and (10) are inverted using a formal development:

$$\begin{cases} T_{G,1} = \left(I + \frac{\alpha}{P} \frac{\partial}{\partial x} \right)^{-1} T_s = T_s + \sum_{k=1}^{\infty} \left(-\frac{\alpha}{P} \right)^k \frac{\partial^k T_s}{\partial x^k} \\ T_{G,2} = \left(I - \frac{1}{P} \frac{\partial}{\partial x} \right)^{-1} T_s = T_s + \sum_{k=1}^{\infty} \left(\frac{1}{P} \right)^k \frac{\partial^k T_s}{\partial x^k} \end{cases} \quad (18)$$

The convergence of the series is guaranteed when $P > 1$; as P is much greater than unity, it is possible to truncate the development at the second-order term, thus obtaining the following approximations:

$$\begin{cases} T_{G,1} \cong T_s - \frac{\alpha}{P} \frac{\partial T_s}{\partial x} + \left(\frac{\alpha}{P} \right)^2 \frac{\partial^2 T_s}{\partial x^2} \\ T_{G,2} \cong T_s + \frac{1}{P} \frac{\partial T_s}{\partial x} + \left(\frac{1}{P} \right)^2 \frac{\partial^2 T_s}{\partial x^2} \end{cases} \quad (19)$$

Combining eq. (19) and (8), the following pseudo-homogeneous heat balance is obtained:

$$\left(\frac{1}{P_{ax}} + \frac{1 + \alpha^2}{2P} \right) \frac{\partial^2 T_s}{\partial x^2} + \frac{1 - \alpha}{2} \frac{\partial T_s}{\partial x} + \frac{a_v (-\Delta H) H/2}{\rho_{G,0} v_0 c_{p,G}} \frac{r_{S,1} + r_{S,2}}{2} \varphi(x) = \tau \frac{\partial T_s}{\partial t} \quad (20)$$

which has to be solved with eq. (11)-(14) in order to obtain the temperature and concentration profiles. As it was shown by Edouard et al. (2004) the first term of eq. (20) involves an effective axial conductivity which is given by:

$$\frac{1}{P_{ax}} + \frac{1 + \alpha^2}{2P} = \frac{\lambda_{eff}}{\rho_{G,0} v_0 c_{p,G} H/2} \Rightarrow \lambda_{eff} = \lambda_{ax}^S + \frac{1 + \alpha^2}{2} \frac{(\rho_{G,0} v_0 c_{p,G})^2}{h a_v} \quad (21)$$

When $\alpha = 1$ (i.e. no dilution occur), λ_{eff} reduces to the well known expression given

by Vortmeyer and Schäfer (1974).

The boundary conditions for the thermal balance equation is modified as now there are no more two gas-phase first-order thermal balance equations and one solid-phase second-order thermal balance equation, but just eq. (20). As a consequence, the boundary conditions given by eq. (17) are expressed using eq. (19) and truncating the developments above $1/P$:

$$\begin{cases} x = 0, & T_s - \frac{\alpha}{P} \frac{\partial T_s}{\partial x} = T_{G,0} \\ x = 1, & (1 + N') \left(T_s + \frac{1}{P} \frac{\partial T_s}{\partial x} - T_{G,0} \right) = \alpha \left(T_s - \frac{\alpha}{P} \frac{\partial T_s}{\partial x} - T_{G,0} \right) + \frac{\dot{Q}_{ext}}{\rho_{G,0} v_0 c_{p,G} S} \end{cases} \quad (22)$$

It is important to highlight that the boundary conditions (17) after the change of variables (19) are more than those required by eq. (20) and thus the conditions over T_s are ignored.

The contribution of the second reactor to the reaction rate, namely $r_{s,2}$ may be neglected: if the reactor is fully ignited, the reaction may be assumed instantaneous and occurring in the upstream monolith at $x = \xi$. Even when the reactant conversion decreases and the reaction front starts moving in the upstream monolith, the contribution of the downstream monolith may be neglected. If the reaction front reaches the downstream monolith (and thus its contribution to the reaction term in the mass balance cannot be neglected any more) it means that the reaction is almost extinct. Figure 3 shows a comparison between the solid temperature profiles that are obtained in the reactor when the contribution of the downstream monolith is neglected or not: no differences are obtained in the prediction when the reactor is fully ignited, while there is a slight difference when the reactant conversion starts decreasing. This simplification will allow us to give to the system of equations a useful structure for the synthesis of the observer.

A first order kinetic may be generally assumed:

$$r_{s,1} = k_0 e^{-\frac{E_a}{RT_s}} c_s = k_0 e^{-\frac{E_a}{RT_s}} \frac{\omega_{s,1} \rho_G}{M} \quad (23)$$

Because of these assumption, eq. (20) may be rewritten:

$$\left(\frac{1}{P_{ax}} + \frac{1+\alpha^2}{2P} \right) \frac{\partial^2 T_s}{\partial x^2} + \frac{1-\alpha}{2} \frac{\partial T_s}{\partial x} + P \Delta T_{ad} \frac{k_0}{k_D} \frac{\omega_{s,1}}{\omega_{G,0}} \frac{1}{2} e^{-\frac{E_a}{RT_s}} = \tau \frac{\partial T_s}{\partial t} \quad (24)$$

where

$$\Delta T_{ad} = \frac{\omega_{G,0} (-\Delta H)}{Mc_{p,G}} \quad (25)$$

The finite frequency in the RFR is responsible for a deviation with respect to the prediction based on the countercurrent model; the simple correction introduced by Edouard et al. (2004) can be used to take into account the finite flow reversal frequency.

High Gain Observer

A model-based control or supervision strategy requires the knowledge of the state of the process; this may be achieved by using physical sensors. In many cases the number and type of sensors is limited due to cost consideration and physical constraints. An observer for a process described by a non-linear dynamic system

$$\dot{x} = f(x, u) \quad (26)$$

whose observations are given by

$$y = g(x, u) \quad (27)$$

is another dynamic system,

$$\dot{\hat{x}} = f(\hat{x}, u) + \kappa(y - g(\hat{x}, u)) \quad (28)$$

having the property that the estimation error, given by

$$e = x - \hat{x} \quad (29)$$

converges to zero, independent by the state and the input. The differential equation for the error e can thus be used to study the behaviour of the observer. This equation is given by

$$\dot{e} = x - \hat{x} = f(x, u) - f(x - e, u) - \kappa(g(x, u) - g(x - e, u)) \quad (30)$$

Suppose that by a proper choice of $\kappa(\cdot)$ the eq. (30) can be made asymptotically stable, i.e. an equilibrium state is reached for which

$$\dot{e} = 0 \quad (31)$$

Then, in equilibrium, eq. (30) becomes

$$0 = f(x, u) - f(x - e, u) + \kappa(g(x - e, u) - g(x, u)) \quad (32)$$

Since the right-hand side of eq. (30) becomes zero when $e = 0$, independent of x and u , $e = 0$ is an equilibrium state of eq. (31). This implies that if $\kappa(\cdot)$ can be chosen to achieve asymptotic stability, the estimation error converges to zero.

The Kalman filter is often proposed in the literature for selecting the gain of an observer; the numerical difficulties involved in the design of Kalman filter based observers can render the on-line estimation very time-consuming. A different approach was used in this work, deriving the observer from the high gain techniques (Bonard and Hammouri, 1991; Deza et al., 1992; Farza et al., 1998; Gauthier et al., 1992; Gauthier and Kupka, 1994). The calculation of the proposed observer gain does not require to solve any differential equation and its calibration, based on a canonical form, is very simple. This section is organised as follows: first, we use the finite difference method to approximate the reactor model by a system of ordinary differential equations; next, the resulting model is re-ordered to get a particular structure which allows to synthesize the observer.

Space discretisation of the system: finite difference method

The heat balance equation (24) was discretised over 200 points: the same numbers of points were used both in the inert and in the catalytic monoliths, leading to different space discretisation:

- for $1 \leq i \leq 100$ and $102 \leq i \leq 200$:

$$\begin{cases} \left. \frac{\partial T_S(x,t)}{\partial x} \right|_i = \frac{T_S(x_i,t) - T_S(x_{i-1},t)}{\Delta x_k} \\ \left. \frac{\partial^2 T_S(x,t)}{\partial x^2} \right|_i = \frac{T_S(x_{i+1},t) - 2T_S(x_i,t) + T_S(x_{i-1},t)}{\Delta x_k^2} \end{cases} \quad (33)$$

- for $i = 101$:

$$\begin{cases} \left. \frac{\partial T_S(x_{101},t)}{\partial x} \right| = \frac{T_S(x_{101},t) - T_S(x_{100},t)}{\Delta x_1} \\ \left. \frac{\partial^2 T_S(x_{101},t)}{\partial x^2} \right| = \frac{T_S(x_{102},t)}{\Delta x_2^2} - \frac{(\Delta x_1 + \Delta x_2)T_S(x_{101},t)}{\Delta x_2^2 \Delta x_1} + \frac{T_S(x_{100},t)}{\Delta x_2 \Delta x_1} \end{cases} \quad (34)$$

where $\Delta x_k = x_i - x_{i-1}$. The temperatures in the points x_0 and x_{201} are given by the discretisation of the boundary conditions. The discretised temperature profile is denoted by:

$$X(t) = (X_1(t), X_2(t), \dots, X_{200}(t))^T \quad (35)$$

where

$$X_i(t) = T_S(x_i, t) \quad (36)$$

$(T_S(x_1, t), \dots, T_S(x_{100}, t))^T$ corresponds to the non reactive monolith compartment ($\Delta x_k = \Delta x_1$) and $(T_S(x_{101}, t), \dots, T_S(x_{200}, t))^T$ corresponds to the reactive monolith compartment ($\Delta x_k = \Delta x_2$). The discretisation of the eq. (24), using the eq. (11) and (13) to calculate the concentration at the solid surface, yields to the system:

$$\dot{X}(t) = A(\alpha(t))X(t) + B(\alpha(t), X(t))U(t) \quad (37)$$

where

$$U(t) = (T_{G,0}, Q_{ext}(t), \Delta T_{ad}(t))^T,$$

$$A(\alpha(t)) = \begin{pmatrix} a_4(t) & a_1(t) & 0 & \dots & \dots & \dots & 0 \\ a_3(t) & a_2(t) & a_1(t) & \dots & \dots & \dots & 0 \\ 0 & \ddots & \ddots & \ddots & \dots & \dots & 0 \\ \vdots & \ddots & a_{3c}(t) & a_{2c}(t) & a_1(t) & 0 & \vdots \\ \vdots & \ddots & 0 & \ddots & \ddots & \ddots & 0 \\ 0 & \ddots & \ddots & 0 & a_3(t) & a_2(t) & a_1(t) \\ 0 & \dots & \dots & \dots & 0 & a_3(t) & a_5(t) \end{pmatrix},$$

$$B(\alpha(t)) = \begin{pmatrix} b_1(t) & 0 & 0 \\ 0 & 0 & 0 \\ \vdots & \vdots & \vdots \\ 0 & 0 & 0 \\ 0 & 0 & \frac{P}{2\tau} \frac{k_0}{k_D} e^{-\frac{E_a}{RT_s(x_{101})}} M_c \\ \vdots & \vdots & \vdots \\ 0 & 0 & \frac{P}{2\tau} \frac{k_0}{k_D} e^{-\frac{E_a}{RT_s(x_{199})}} M(x_{199}) \\ b_2(t) & b_3(t) & \frac{P}{2\tau} \frac{k_0}{k_D} e^{-\frac{E_a}{RT_s(x_{200})}} M(x_{200}) \end{pmatrix}$$

and the coefficients are given in Appendix 1.

The canonical structure of the system

The aim of the observer is to provide a reliable on-line estimation of the inlet pollutant concentration, i.e. the ΔT_{ad} , due to the proportionality relationship given by eq. (25). Following the same approach of Edouard et al. (2004), the ΔT_{ad} is considered the response of a second order system:

$$\begin{cases} \frac{d}{dt} \Delta T_{ad} = \zeta(t) \\ \frac{d}{dt} \zeta(t) = v(t) \end{cases} \quad (38)$$

where $v(t)$ is an unknown, but bounded signal.

The aim of our observer is not only to estimate the inlet pollutant concentration also when the conversion is no longer one. In this conditions, i.e. mass transfer controlled reaction, the model becomes dependent from the kinetic parameter, which may be unknown due to:

- change of the type of the pollutant which is fed to the reactor;
- catalyst deactivation or aging;
- poorly understood kinetic parameters.

As a consequence, the observer should be able to estimate also the kinetic parameters of the catalyst. Because of first order kinetic assumption, two are the kinetic parameters, namely the frequency factor and the activation energy. The assumption of first order kinetic does not limit the application of our observer as almost any reaction rate may be approximated by a first order equation in a certain range of composition; moreover, now the parameters of the first order equation, changes due to the estimation. For sake of simplicity we decided to keep constant the value of the activation energy and to estimate only the frequency factor; also this assumption is not limitative as it is always possible to calculate a frequency factor (for a fixed value of activation energy) to get the value of any kinetic constant.

The formulation of this observer requires a particular structure called canonical form; the following notations are used to re-order the system (37) into this form:

$$\begin{cases} z^1(t) = (z_1^1(t), \dots, z_{100}^1(t))^T = (X_1(t), \dots, X_{100}(t))^T \\ z^2(t) = (z_1^2(t), z_2^2(t), z_3^2(t), z_4^2(t))^T = \left(X_{101}(t), \Delta T_{ad}(t), \zeta(t), \frac{k_0}{k_D} \right)^T \\ z^3(t) = (z_1^3(t), \dots, z_{99}^3(t))^T = (X_{200}(t), \dots, X_{102}(t))^T \end{cases} \quad (39)$$

Due to the structure of the equations, our observer will not estimate the frequency factor k_0 but the ratio k_0/k_D . With these notations, the system (37) can be rewritten as:

$$\begin{cases} \dot{z}^1 = a_1(t) A^1 z^1(t) + G^1(T_{G,0}, \alpha(t), y_2(t), z^1(t)) \\ \dot{z}^2 = A^2 z^2(t) + G^2(\alpha(t), y_2(t), z_{100}^1(t), z_{99}^3(t), z^2(t)) \\ \dot{z}^3 = A^3 z^3(t) + G^3(\alpha(t), y_2(t), z^2(t), z^3(t), T_{G,0}, Q_{ext}) \end{cases} \quad (40)$$

The matrices A and G are given in Appendix 2.

The state measurements that are used to estimate the state of the system are:

$$\begin{cases} y_1(t) = X_1(t) = T_S(x_1, t) \\ y_2(t) = X_{101}(t) = T_S(x_{101}, t) \\ y_3(t) = X_{200}(t) = T_S(x_{200}, t) \end{cases} \quad (41)$$

i.e. the temperature at the inlet of the non-reactive monolith, the temperature at the inlet of the reactive monolith and the temperature at the outlet of the upstream reactive monolith.

Observer design for on-line estimation of the unknown pollutant concentration

The observer for the system (40) takes this form:

$$\begin{cases} \dot{\hat{z}}^1(t) = a_1(t)A^1\hat{z}^1 + G^1(\hat{z},t) - a_1(t)\Delta_{1\Omega}K^1(\hat{z}_1^1 - y_1(t)) \\ \dot{\hat{z}}^2(t) = A^2\hat{z}^2 + G^2(\hat{z},t) - \Lambda\Delta_\theta K(\hat{z}_1^2 - y_2(t)) \\ \dot{\hat{z}}^3(t) = a_3(t)A^3\hat{z}^3 + G^3(\hat{z},t) - a_3(t)\Delta_{3\Omega}K^3(\hat{z}_1^3 - y_3(t)) \\ y_1(t) = z_1^1(t) = T_S(x_1, t) \\ y_2(t) = z_1^2(t) = T_S(x_{101}, t) \\ y_3(t) = z_1^3(t) = T_S(x_{200}, t) \end{cases} \quad (42)$$

where the observers for the states \hat{z}^1 and \hat{z}^3 are the same described by Edouard et al.

(2004), i.e. $K^1 = \begin{pmatrix} K_1^1 \\ \vdots \\ K_{100}^1 \end{pmatrix}$ and $K^3 = \begin{pmatrix} K_1^3 \\ \vdots \\ K_{99}^3 \end{pmatrix}$ are such that the matrices

$$\bar{A}^1 = \begin{pmatrix} K_1^1 & 1 & 0 & 0 \\ \vdots & 0 & \ddots & \vdots \\ K_{99}^1 & 0 & \cdots & 1 \\ K_{100}^1 & 0 & \cdots & 0 \end{pmatrix}, \text{ and } \bar{A}^3 = \begin{pmatrix} K_1^3 & 1 & 0 & 0 \\ \vdots & 0 & \ddots & \vdots \\ K_{98}^3 & 0 & \cdots & 1 \\ K_{99}^3 & 0 & \cdots & 0 \end{pmatrix} \text{ are stable, i.e. the real part of their}$$

eigenvalues are negative, and $\Delta_{1\Omega}$ and $\Delta_{3\Omega}$ are respectively 100x100 and 99x99

matrices having this form: $\Delta_{1\Omega} = \begin{pmatrix} \Omega_1 & \cdots & 0 \\ \vdots & \ddots & \vdots \\ 0 & \cdots & \Omega_1 \end{pmatrix}$, $\Delta_{3\Omega} = \begin{pmatrix} \Omega_3 & \cdots & 0 \\ \vdots & \ddots & \vdots \\ 0 & \cdots & \Omega_3 \end{pmatrix}$. The proof of

the convergence of this observer was given in Edouard et al. (2004).

The observer for the state \hat{z}^2 was taken from Hammouri and Farza (2003); they considered a system with the following canonical structure:

$$\begin{cases} \dot{r} = F(u, r) \\ y = Cr \end{cases} \quad (43)$$

where $F(u, r) = \begin{pmatrix} F^1(u, r) \\ \vdots \\ F^q(u, r) \end{pmatrix}$, $r = \begin{pmatrix} r^1 \\ \vdots \\ r^q \end{pmatrix}$ and each function $F^i(u, r)$, $i=1, \dots, q-1$ satisfies the

following structure:

$$F^i(u, r) = F^i(u, r^1, \dots, r^{i+1}) \quad (44)$$

with the following rank condition:

$$\text{Rank} \left(\frac{\partial F^i(u, r)}{\partial r^{i+1}} \right) = n_{i+1} \quad (45)$$

The following functions are introduced:

$$\begin{aligned} \Phi^1(u, r^1) &= r^1 \\ \Phi^k(u, r^1, \dots, r^k) &= \frac{\partial \Phi^{k-1}(u, r^1, \dots, r^{k-1})}{\partial r^{k-1}} F^{k-1}(u, r^1, \dots, r^k); 2 \leq k \leq q \end{aligned} \quad (46)$$

The observer for the system (43), (44), (45) takes the following form:

$$\dot{\hat{r}} = F(u, \hat{r}) - \Lambda(u, \hat{r}) \Delta_\theta K (C\hat{r} - y) \quad (47)$$

where F is given in (43), $\Lambda(u, \hat{r}) = \left[\left(\frac{\partial \Phi(u, \hat{r})}{\partial r} \right)^T \frac{\partial \Phi(u, \hat{r})}{\partial r} \right]^{-1} \left(\frac{\partial \Phi(u, \hat{r})}{\partial r} \right)^T$ with

$$\Phi = \begin{pmatrix} \Phi^1 \\ \vdots \\ \Phi^q \end{pmatrix}, \Delta_\theta = \begin{pmatrix} \theta I_{n_1} & 0 & \dots & 0 \\ 0 & \theta^2 I_{n_1} & 0 & \vdots \\ \vdots & & \ddots & 0 \\ 0 & \dots & 0 & \theta^q I_{n_1} \end{pmatrix}, I_{n_1} \text{ is the } n_1 \times n_1 \text{ identity matrix.}$$

K is a $qn_1 \times n_1$ constant matrix such that $(A - KC)$ is a stability matrix.

In our system (42):

$$\begin{aligned} r^1 &= z_1^2 \\ r^2 &= \begin{pmatrix} z_2^2 \\ z_3^2 \end{pmatrix} \\ r^3 &= z_4^2 \end{aligned} \quad (48)$$

thus $q = 3$ and $n_1 = 1$.

Validation of the observer

Due to the low thermal capacity of the monolithic support, a low value of switching time is required to allow autothermal operation. A value of 16 s is used and is kept constant; this low value justifies also the use of the analogy with the countercurrent reactor which is at the basis of our reactor model and thus of our observer. The pollutant is xylene; the kinetic parameters used in the model are shown in Table 1. The lid of the rig is not perfectly airtight and thus a small amount of fresh air ($\alpha = 0.95$) is aspirated in the central chamber of the reactor. The sampling frequency of the thermocouples is 0.025 Hz. The following analysis was repeated also using a sampling frequency of 0.25 Hz without significant differences.

Figure 4 shows the comparison between the experimental measured values and the on-line estimation of the inlet xylene concentration and of the solid temperatures at the inlet of the non-reactive monolith, at the inlet of the reactive monolith and at the outlet of the upstream reactive monolith. The experimental values are the same used by Edouard et al. (2004) to validate their observer. The aim of this comparison is to state, first of all, the adequacy of our observer, when the system is fully ignited. As far as the solid temperatures are concerned, the agreement is excellent: a maximum of 1-2 K in the difference between experimental and estimated values at the boundaries between catalytic and inlet monoliths and at the inlet inert monolith and less than 5 K at the outlet catalytic monolith. Also the inlet concentration is properly estimated, both when stiff changes take place in the steady portions with low response time.

The same comparison is repeated in Figure 5, when the reactor moves towards the extinction. Not only the solid temperatures but also the inlet concentration are properly estimated during this phase. The observer of Edouard et al. (2004), in the same conditions, gives an inlet concentration equal to zero as, being independent from any kinetic parameters, the only condition that can explain the extinction of the

reactor is that the ΔT_{ad} of the feed is zero; moreover that observer is not able to estimate the pollutant conversion. Conversely, the observer we have proposed is able to estimate the conversion of the pollutant, as it is shown in Figure 6. Beside the good estimation of the solid temperature, thus giving the value of the maximum temperature which can be used to prevent catalyst over-heating, pollutant conversion is the other important parameters that has to be known for control purposes.

The “state” which is estimated by the observer is made up of not only by the solid temperature and the inlet concentration, but also by the ratio k_0/k_D . As it has been stated in the previous section where the observer has been described, for sake of simplicity the activation energy has been kept constant and only the frequency factor has been optimised. The results for the experimental run previously considered are shown in Figure 7.

Finally, Figure 8 shows a run where not only the inlet VOC concentration but also the VOC type are changed. Till the first 6000 s xylene is fed to the reactor, and then, for 14000 s, the feed is composed by eptane and, finally, the feed is considered to be composed by buthyl-acetate. The prediction of the observer are obtained using the values of the solid temperatures coming from the numerical simulation of the system, instead of using the experimental values. The agreement between the “real” values and the estimation of the observer is excellent, as well as the velocity in the response of the observer.

Conclusions

The control of a reverse-flow afterburner requires to know both the solid temperature (to prevent catalyst overheating) and the pollutant conversion (to avoid pollutant emission). The proposed observer was demonstrated to give a quick and reliable estimation of the solid temperature and of the pollutant conversion, using

some temperature measurements, even if we have uncertainties on the kinetic parameters. This sensor was checked in a wide range of operating conditions and was demonstrated to fulfil the requirements both when the reactor is fully ignited and when the reaction is approaching extinction and when the type of the pollutant changes. This instrument can thus be used in a state-space based control framework (like LQR or MPC), and this will be the subject of a future work.

References

- Balakotaiah V, Dommeti SMS. Effective models for packed-bed catalytic reactors. *Chemical Engineering Science*. 1999; 54: 1621-1638.
- Bonard G, Hammouri H. A high gain observer for a class of uniformly observable systems. *Proceedings of the 30th IEEE Conference on Decision and Control*, Brighton, England (1991), 1494-1501.
- Deza F, Busvelle E, Gauthier J P, High gain estimation for nonlinear systems. *System & Control Letters*. 1992; 18: 295-299.
- Dufour P, Couenne F, Touré Y. Model predictive control of a catalytic reverse flow reactor. *IEEE Transactions on Control System Technology*. 2003, 11: 705-714.
- Dufour P, Touré Y. Multivariable model predictive control of a catalytic reverse flow reactor. *Computers and Chemical Engineering*. 2004, 28: 2259-2270.
- Edouard D, Schweich D, Hammouri H. Observer design for reverse flow reactor. *AIChE Journal*. 2004, 50: 2155-2166.
- Edouard D, Dufour P, Hammouri H. Observer based multivariable control of a catalytic reverse flow reactor: comparison between LQR and MPC approaches. *Computers and Chemical Engineering*. 2005, *In Press*.
- Eigenberger G. Fixed bed reactors, in: *Ullmann's Encyclopedia of chemical industry*, 1992, VCH, Weinheim.
- Farza M, Hammouri H, Busavon K. A simple observer for a class of nonlinear systems. *Applied Mathematics Letters*. 1998; 11: 27-31.
- Gauthier JP, Hammouri H, Othman S. A simple observer for nonlinear systems. Application to bioreactors. *IEEE Transaction on Automatic Control*. 1992; 37: 875-880.
- Gauthier JP, Kupka AK. Observability and observers for nonlinear systems. *SIAM Journal on Control and Optimisation*. 1994; 32: 975-994.
- Hammouri H, Farza M. Nonlinear observers for local uniform observable systems,

- ESAIM Control Optimisation and Calculus of Variations. 2003; 9: 353-362.
- Matros YS, Bunimovich GA. Reverse-flow operation in catalytic reactors. Catalysis Reviews-Science Engineering. 1996; 38: 1-68.
- Nieken U, Kolios G, Eigenberger G. Limiting cases and approximate solutions for fixed-bed reactors with periodic flow reversal. AIChE Journal. 1995; 48: 191 –1925.
- Ramdani K, Pontier R, Schweich D. Reverse flow reactor at short switching period for VOC combustion. Chemical Engineering Science. 2001, 56: 1531-1539.
- Vortmeyer D, Schäfer RJ. Equivalence of One- and Two-dimensional models for heat transfer processes in packed-beds: one dimensional theory. Chemical Engineering Science. 1974; 29: 485-491.

List of symbols

a_v	specific solid-gas surface area, m^{-1}
c	molar concentration, mol m^{-3}
c_p	specific heat at constant pressure, $\text{J kg}^{-1}\text{K}^{-1}$
E_a	activation energy, J mol^{-1}
h	gas-solid heat transfer coefficient, $\text{J m}^{-2}\text{K}^{-1}\text{s}^{-1}$
H	length of the reactor, m
k_D	gas-solid mass transfer coefficient, m s^{-1}
k_0	frequency factor, m s^{-1}
M	molecular weight, kg mol^{-1}
N'	number of transfer units for heat loss
P	Peclet number for gas-solid heat transfer
P_{ax}	axial Peclet number for heat conduction
\dot{Q}_{ext}	external power supply, J s^{-1}
r	rate of reaction, $\text{mol m}^{-2}\text{s}^{-1}$
R	ideal gas constant, $\text{J K}^{-1}\text{mol}^{-1}$
S	total cross-section of the monolith, m^2
v_0	surface gas velocity, m s^{-1}
t	time, s
T	temperature, K
x	non-dimensional axial reactor coordinate
z	axial reactor coordinate, m

Greeks

α	fraction of feed flow rate
ΔH	reaction enthalpy, J mol^{-1}

ΔT_{ad}	adiabatic temperature rise, K
ε	fraction of open frontal area
λ_{ax}^S	thermal conductivity of the solid, J m ⁻¹ K ⁻¹ s ⁻¹
λ_{eff}	effective thermal conductivity of the solid, J m ⁻¹ K ⁻¹ s ⁻¹
ξ	non-dimensional position of the interface inert-catalyst
ρ	density, kg m ⁻³
τ	heat storage time constant, s
ω	mass fraction

Subscripts and superscripts

0	inlet conditions
1, 2	refers to the upstream or downstream monolith
S	solid phase or solid surface
G	gas phase

Abbreviations

RFR	Reverse-flow reactor
-----	----------------------

Appendix 1

The coefficient of the system (37) are given by:

$$a_1(t) = \frac{\lambda_{eff1}}{\Delta x_k^2}, \quad a_2(t) = -2 \frac{\lambda_{eff1}}{\Delta x_k^2} + \frac{D(t)}{\Delta x_k}, \quad a_3(t) = \frac{\lambda_{eff1}}{\Delta x_k^2} - \frac{D(t)}{\Delta x_k},$$

$$a_4(t) = a_2(t) + a_3(t) \frac{\alpha(t)}{P\Delta x_1} \frac{1}{1 + \frac{\alpha(t)}{P\Delta x_1}},$$

$$a_5(t) = a_2(t) + a_1(t) \frac{1 + N' + \alpha^2(t)}{P\Delta x_2} \frac{1}{(1 + N') \left(1 + \frac{1}{P\Delta x_2}\right) + \frac{\alpha^2(t)}{P\Delta x_2} - \alpha(t)},$$

$$a_{2c} = (\Delta x_1 + \Delta x_2) \frac{\lambda_{eff1}}{\Delta x_1 \Delta x_2^2} + \frac{D(t)}{\Delta x_1}, \quad a_{3c} = \frac{\lambda_{eff1}}{\Delta x_1 \Delta x_2}, \quad b_1(t) = a_3(t) \frac{1}{1 + \frac{\alpha(t)}{P\Delta x_1}},$$

$$b_2(t) = a_1(t) \frac{1 + N' - \alpha(t)}{(1 + N') \left(1 + \frac{1}{P\Delta x_2}\right) + \frac{\alpha^2(t)}{P\Delta x_2} - \alpha(t)},$$

$$b_3(t) = a_1(t) \frac{1}{\rho_{G,0} v_0 c_{p,G} S} \frac{1}{(1 + N') \left(1 + \frac{1}{P\Delta x_2}\right) + \frac{\alpha^2(t)}{P\Delta x_2} - \alpha(t)} \quad \text{with } D(t) = \frac{1 - \alpha(t)}{2\tau},$$

$$\lambda_{eff1} = \frac{1}{\tau P_{ax}} + \frac{1 + \alpha^2(t)}{2P\tau} \quad \text{and } M(x_i) = \prod_{k=1}^i \Lambda(x_k) \cdot \prod_{k=1}^{i-1} K(x_k), \quad \text{with } K(x_i) = 1 + \frac{k_0}{k_D} e^{-\frac{E_a}{RT_s(x_i)}}$$

$$\text{and } \Lambda(x_i) = \frac{\alpha}{\left\{1 + \frac{k_0}{k_D} e^{-\frac{E_a}{RT_s(x_i)}}\right\} \{\alpha + P\Delta x_2\} - P\Delta x_2}, \quad \text{while}$$

$$M_c = \frac{\alpha}{\left\{1 + \frac{k_0}{k_D} e^{-\frac{E_a}{RT_s(x_{101})}}\right\} \{\alpha + P\Delta x_1\} - P\Delta x_1}.$$

Appendix 2

The matrices A^1 and A^3 are 100x100 and 99x99 matrices of the form $\begin{pmatrix} 0 & 1 & \dots & 0 & 0 \\ 0 & 0 & \ddots & 0 & 0 \\ \vdots & \vdots & \ddots & 1 & 0 \\ \vdots & \vdots & \ddots & 0 & 1 \\ 0 & 0 & \dots & 0 & 0 \end{pmatrix}$;

A^2 is a 4x4 matrix defined by $\begin{pmatrix} 0 & \frac{P}{2\tau} z_4^2 (t - \Delta t) e^{-\frac{E_a}{Rz_1^2}} M_c & 0 & 0 \\ 0 & 0 & 1 & 0 \\ 0 & 0 & 0 & 0 \\ 0 & 0 & 0 & 0 \end{pmatrix}$, where Δt is the time

interval and z_1^2 can be replaced by the measured value y_2 in order to obtain the canonical form.

The arrays G are given by:

$$G^1(z, t) = \begin{pmatrix} G_1^1(z, t) \\ G_2^1(z, t) \\ \vdots \\ G_{100}^1(z, t) \end{pmatrix} = \begin{pmatrix} a_4(t)z_1^1 + b_1 T_{G,0} \\ a_3(t)z_1^1 + a_2(t)z_2^1 \\ \vdots \\ a_3(t)z_{99}^1 + a_2(t)z_{100}^1 + a_1(t)y_2 \end{pmatrix}$$

$$G^2(z, t) = \begin{pmatrix} G_1^2(z, t) \\ G_2^2(z, t) \\ G_3^2(z, t) \\ G_4^2(z, t) \end{pmatrix} = \begin{pmatrix} a_{3c}(t)z_{100}^1 + a_{2c}(t)z_1^2 + a_1(t)z_{99}^3 \\ 0 \\ 0 \\ 0 \end{pmatrix}$$

$$G^3(z, t) = \begin{pmatrix} G_1^3(z, t) \\ G_2^3(z, t) \\ \vdots \\ G_{99}^3(z, t) \end{pmatrix} = \begin{pmatrix} a_5(t) + b_2(t)T_{G,0} + b_3(t)Q_{ext} \\ a_1(t)z_1^3 + a_2(t)z_2^3 \\ \vdots \\ a_1(t)z_{97}^3 + a_2(t)z_{98}^3 \\ a_1(t)z_{98}^3 + a_2(t)z_{99}^3 + a_3(t)y_2 \end{pmatrix} + \begin{pmatrix} M(x_{200}) \\ M(x_{199}) \\ \vdots \\ M(x_{103}) \\ M(x_{102}) \end{pmatrix}$$

List of Tables

Table 1 Values of the kinetic parameters of some VOC considered in the simulations.

Table 1

	Xylene	Eptane	Buthyl-acetate
$k_0, \text{m s}^{-1}$	2400	50	500
$E_a, \text{J mol}^{-1}$	47750	43000	59000

List of Figures

- Figure 1* Main geometrical characteristics of the RFR ($l_1 = 355$ mm, $l_2 = 75$ mm, $l_3 = 150$ mm)
- Figure 2* The countercurrent reactor model.
- Figure 3* Comparison between the solid temperature profiles when the contribution of the downstream catalytic monolith is considered (lines) or not (symbols) for different pollutant concentration of the inlet stream.
- Figure 4* Comparison between the experimental measured values (symbols) and the on-line estimation (solid line) of the inlet xylene concentration, given as ΔT_{ad} (upper graph) and of the solid temperatures (lower graph) at the inlet of the non-reactive monolith (x_1), at the inlet of the reactive monolith (x_{101}) and at the outlet of the upstream reactive monolith (x_{200}). The reactor is fully ignited.
- Figure 5* Comparison between the experimental measured values (symbols) and the on-line estimation (solid line) of the inlet xylene concentration (upper graph) and of the solid temperatures (lower graph) at the inlet of the non-reactive monolith (x_1), at the inlet of the reactive monolith (x_{101}) and at the outlet of the upstream reactive monolith (x_{200}). The reactor is approaching extinction.

Figure 6 Comparison between the experimental measured values (symbols) and the on-line estimation (solid line) of the conversion of xylene concentration.

Figure 7 Time evolution of the ratio k_0/k_D as predicted by the observer.

Figure 8 Comparison between the simulated values (solid line) and the observer estimation (symbols) of the inlet VOC concentration when both the VOC and its concentration change.

Figure 1

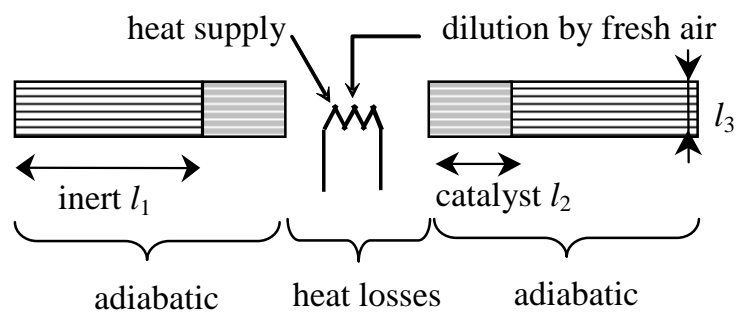


Figure 2

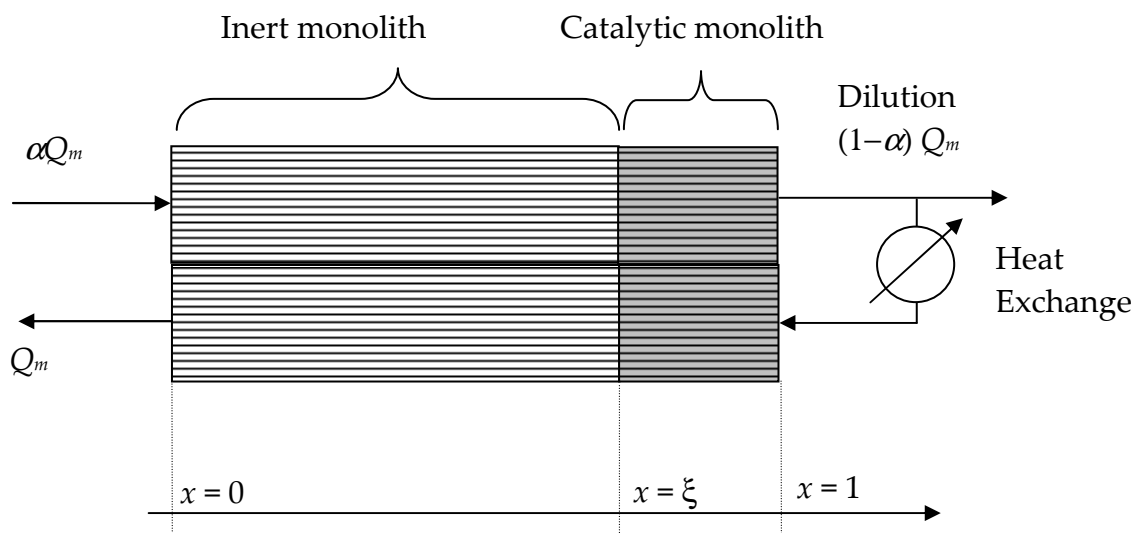


Figure 3

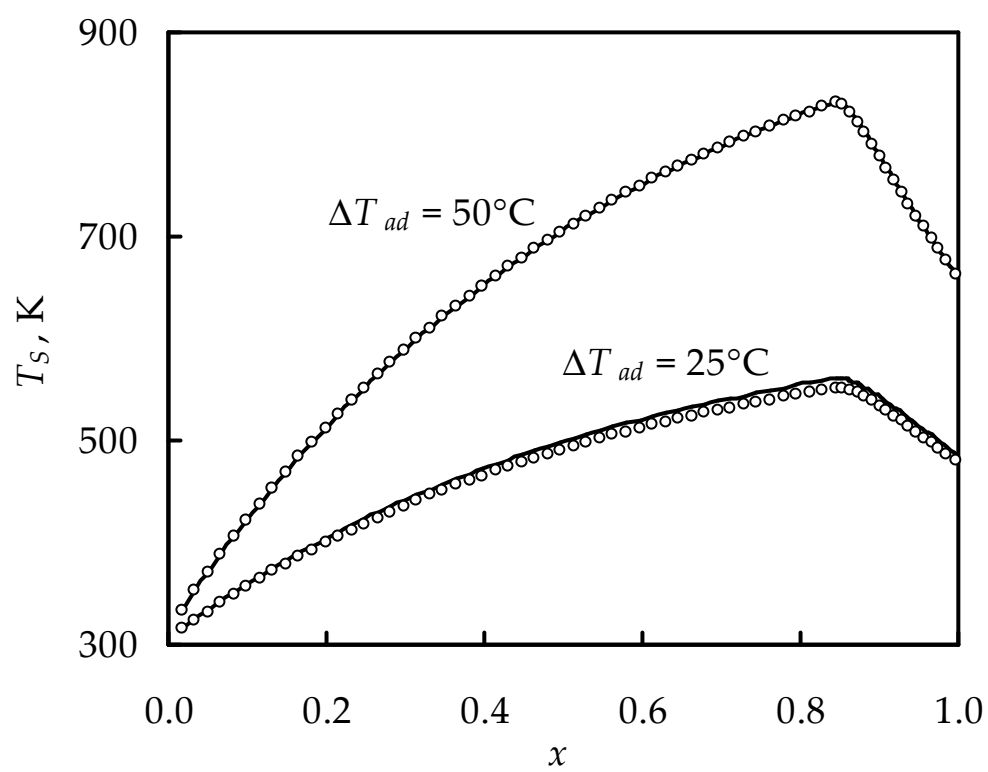


Figure 4

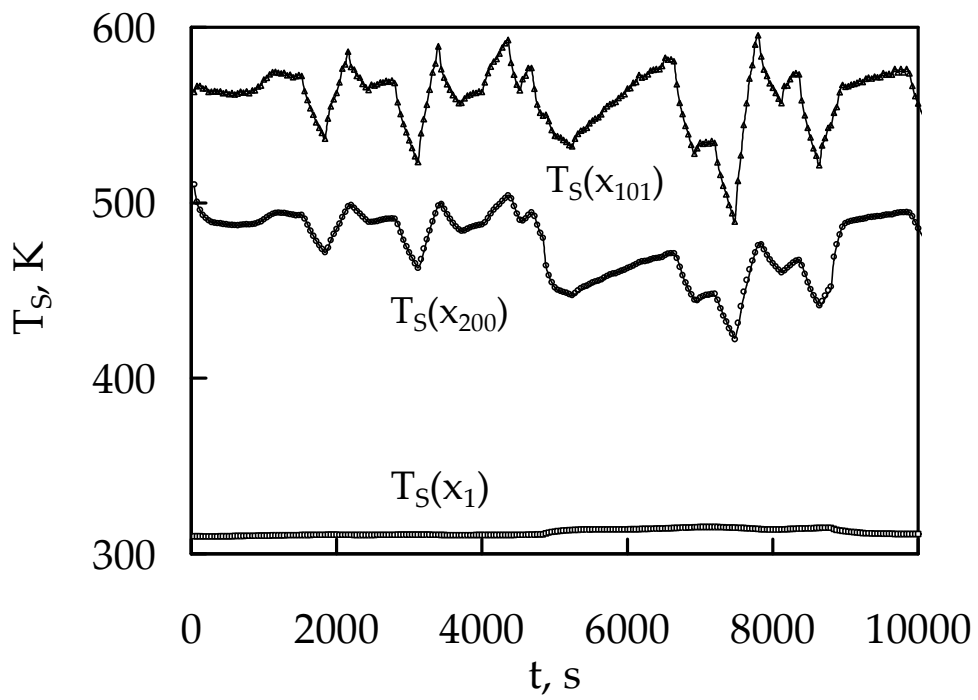
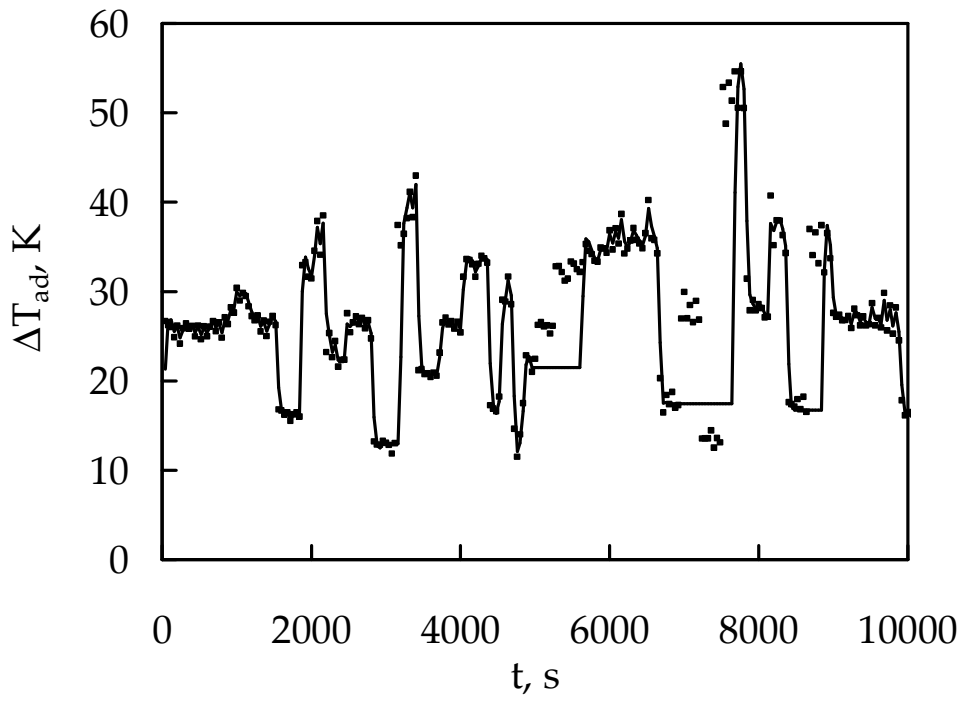


Figure 5

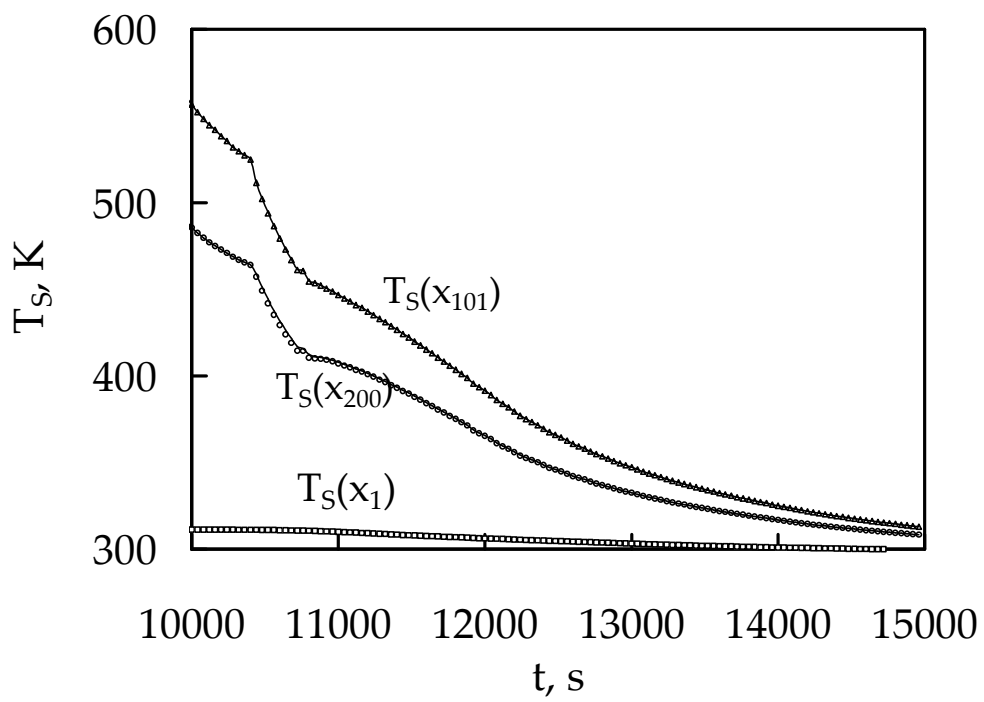
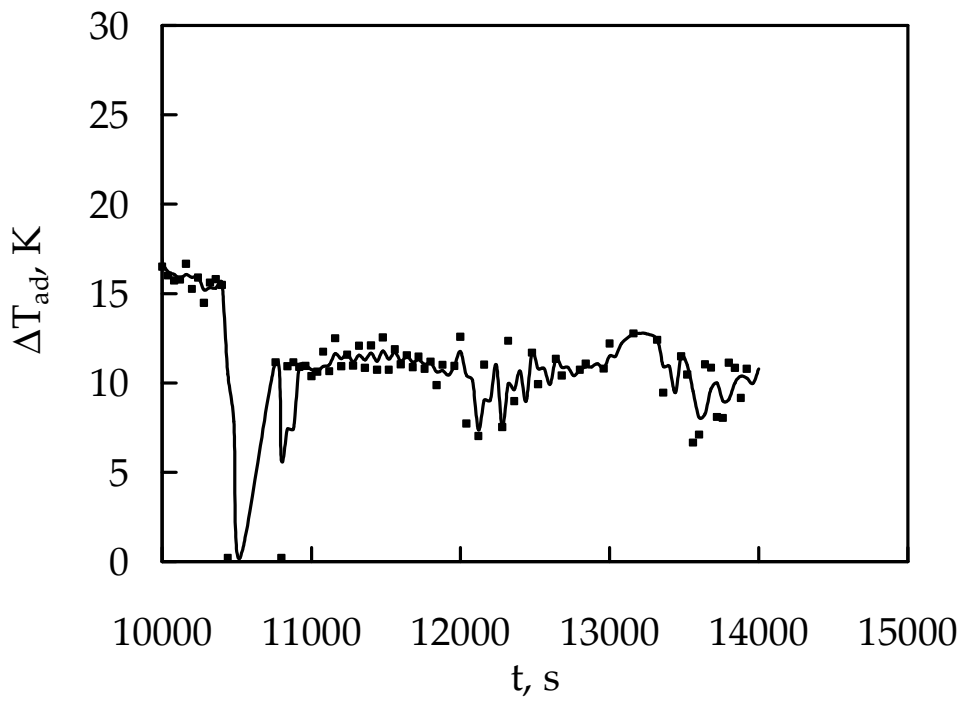


Figure 6

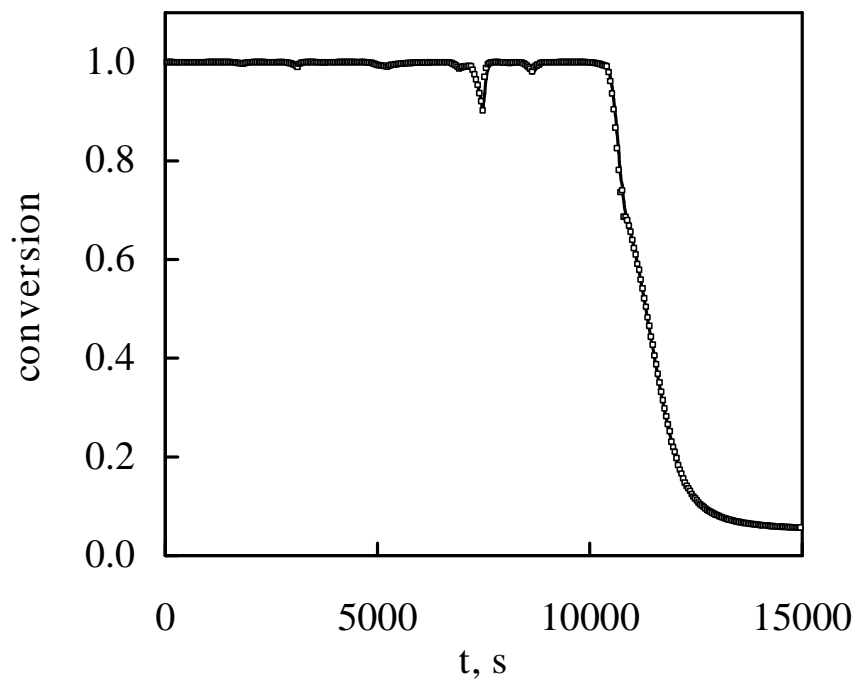


Figure 7

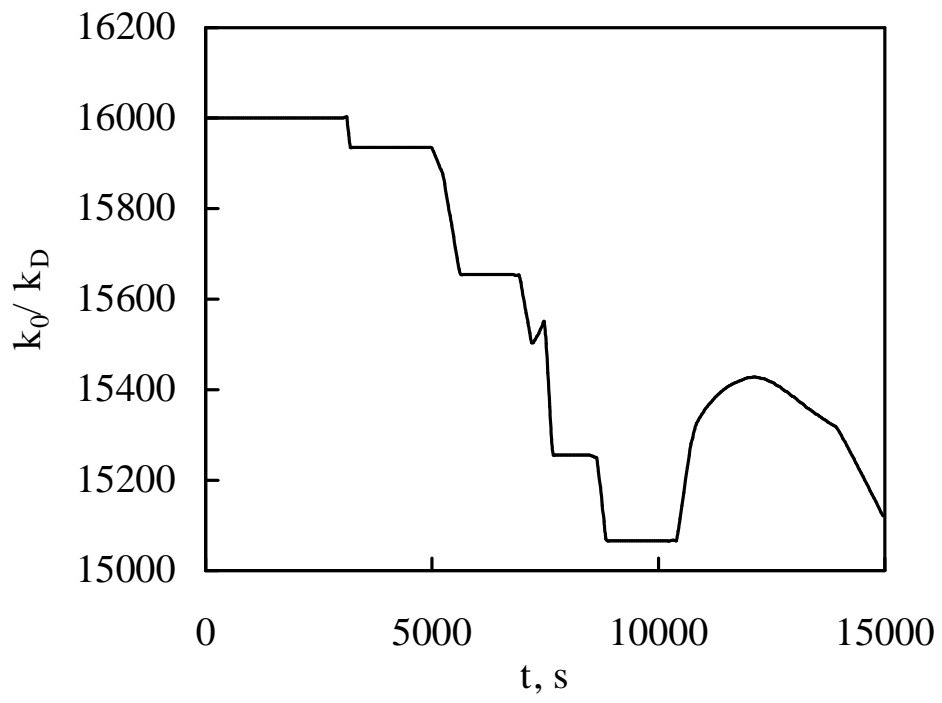


Figure 8

